Patterns of Nuclear Rotational Excitation[1]

JOHN O. RASMUSSEN

Department of Chemistry, Yale University, New Haven, Connecticut 06520

Nature repeats her favorite designs on vastly differing scales, as in the astronomical vastness of the galaxies, the smaller planetary solar system, and the submicroscopic atoms. Going down yet another five orders of magnitude in size we find again the repeated design in nuclear systems, a collection of bodies, the neutrons and protons, circulating in a common attractive central force field. Galactic and nuclear systems differ from the others in that the binding field arises from attraction between near equals, whereas planetary and atomic systems are dominated by attraction of a massive central body. In the smallest two systems the magic numerology of quantization enters, giving rise to particularly stable numbers of particles, the noble gas atomic numbers (2, 10, 18, 36, 54, and 86) on the one hand and the nucleon closed shell numbers (2, 8, 20, 28, 50, 82, and 126) on the other.

For particle numbers differing by one from these special numbers the spectra of low-lying electronic (or nucleonic) excitation are especially simply understood in terms of quantum states of one particle moving in an appropriate central potential. For atoms, ions, or nuclei as we move further away from the numbers of stability the energy spectra become considerably more complex and difficult to calculate by theoretical models. Many semiempirical rules, such as Hund's rules for atomic systems, have been developed for these complex systems. In nuclei as the neutron and proton numbers are both made sufficiently different from a closed-shell number a profound reorganization of the nuclear system takes place, with a prolate spheroidal shape replacing the spherical. In these egg-shaped nuclei nature seems bent on imitating linear molecules, replete with relatively closely spaced rotational band structure superimposed on more widely spaced vibronic excitation states. The vibronic excitations are interpreted in terms of molecular orbitals in a potential of cylindrical, not spherical, symmetry.

It is the purpose of this review to consider the ways by which rotational energy is imparted to nuclear products from many processes. In this respect we are dealing with the nuclear analogies to processes of central concern in modern physical chemistry—the processes of partitioning available energy among rotational and other degrees of freedom.

In sections IIA,B we deal with relative transition intensities to various rotational states in nuclei following radioactive decay processes. It is seen that these relative intensity relationships come from purely geomet-

rical considerations identical with those for radiative transitions in diatomic molecules. In particular the geometrical factors have a dependence on the K quantum number, the projection of angular momentum along the long axis, and thus the intensity ratios afford a means of determining the K quantum number.

In section IIC we examine the rotational energy distribution after a spontaneous two-body breakup and see its direct relationship to the state of motion in the "activated complex" transition state. The principles would carry over in close analogy to the breakup of a triatomic molecule into an atom plus a diatomic molecule. The rotational energy pattern of the diatomic product could provide a snapshot of the conformation and vibrational amplitudes in the transition complex.

Section IIIA treats the transfer of translational energy to rotational energy in collisions, at low enough energies that the only coupling comes from the electrostatic interaction of a point charge with a quadrupole. The exact molecular analogy would be the collision of a monatomic ion with a diatomic molecule ion at energies sufficiently low that the electron clouds of the ions do not touch. Sections IIIB,C deal with the same translational–rotational energy transfer but for higher collision energies, where the nuclear surfaces may make contact, either without (B) or with (C) a reaction taking place. Analogs would be energetic ion–molecule reactions in which electron transfer does not (B) or does (C) take place.

In section IIID we consider reaction processes which are the inverse of the two-body breakup treated in section IIC. Finally in section IIIE we advance the new notion that rotational energies imparted to fission fragments may be handled by the same two-body breakup ideas as α decay, treated in section IIC.

It is to be hoped that these discussions of nuclear processes will suggest to those in molecular studies the wealth of fundamental information that can follow from careful measurement of rotational energy distributions in reaction products.

Since the focus of this Account is on rate processes and intensities, we have tried to avoid digressing to show and discuss actual level schemes and the degree to which rotational motion may be separated from vibronic in various nuclei. For those interested in this matter an Appendix showing level schemes has been included.

I. Milestones in the Study of Nuclear Rotation

Beginning around 1953 it became clear that in two broad regions of the periodic table nuclei have large prolate deformations, rather than the spherical equilibrium shapes of most light nuclei.[2a] One region encom-

passes nuclei with neutron number between 90 and ~114 and the other, those above 134. The light nuclei near ^{24}Mg also constitute a smaller island of deformation. Within these regions nuclei exhibit many properties closely analogous to those of diatomic molecules. A most striking property is the grouping of energy levels into closely spaced rotational bands, with moments of inertia ranging from ~10% to nearly that of the rigid body value ($\sim^2/_5MR^2$). A. Bohr in 1952 laid the groundwork[2b] and predicted the existence of rotational bands in nuclei. Much of the most direct early evidence of nuclear rotational bands came from results of the high-resolution α spectroscopy research done by Asaro and Perlman.[3] In their studies they used a large magnetic spectrograph to bend and focus the energetic helium ions ejected by nuclei in so-called α radioactivity. They observed for even–even nuclei (those with even numbers of protons and neutrons, respectively) from around ^{224}Th on up α line spectra populating a rotational band of only even angular momenta (as in the ^{16}O–^{16}O molecule) based on the ground state ($I = 0, 2, 4,$). These ground bands of even nuclei stand out clearly, since there are seldom any other bands that come low enough in energy to confuse interpretation.

α radioactivity is prevalent only in the heaviest elements, so it remained for other techniques to discover and map the other large continent of deformation lying between samarium and osmium. Huus and Zupancic[4] soon showed that the egg-shaped deformations of these nuclei were all so large that the first excited rotational states could be excited *via* an electric quadrupole interaction with a passing projectile ion well below the Coulomb barrier energy needed for a nuclear collision. This technique, Coulomb excitation, became a powerful general tool for mapping the first excited states of stable deformed nuclei and measuring their deformations. The processes of β decay and isomeric electromagnetic decay also revealed bands, though less generally than α decay and Coulomb excitation. An interesting early example is the β decay (emission of a negative electron and antineutrino) scheme of natural ^{176}Lu (half-life 3×10^{10} years) determined[5] by Arnold and Sugihara in 1953; they observed γ rays defining the ^{176}Hf daughter ground band of spins 0, 2, 4, 6. The exceedingly long lifetime showed the importance of the K quantum number[6] selection rules; although the angular momentum change in the β decay is only one unit, the K change is seven units, thus inhibiting the decay some 12 orders of magnitude over that normally expected.

We conclude the historical preliminaries by noting the precedent-setting applications of heavy ion beams ($Z \geqslant 5$) in pushing the knowledge of rotational bands to record high-spin values. In 1959 oxygen ions below the Coulomb barrier were found effective[7] in exciting by a single collision several quanta of rotational angular momentum, pushing knowledge of the ground rotational band of ^{238}U up through the spin 12 member at 1.1 MeV. Later, following pioneering work with helium ions in Amsterdam[8] a research group in Berkeley[9] fired heavy ions *above* the Coulomb barrier at deformed rare-earth nuclei carrying tens of units of angular momentum into the reaction intermediate, the compound nucleus. After evaporation of neutrons and emission of γ rays by myriad paths into the rotational bands it was found still quite feasible to identify the ground band transitions. In this fashion have been mapped the rotational bands of a great number of neutron-deficient deformed even–even nuclei of the Dy to Os region. Record high spin levels of 18+ have been identified in ^{170}Hf and ^{172}Hf by this powerful technique.[9]

An excellent presentation of our present understanding of nuclear sizes and shapes is to be found in a recent article by Baranger and Sorensen.[10]

II. Rotational Intensity Patterns in Radioactivity

A. Qualitative Deductions from α Decay of Odd-Mass Nuclei. That the levels of odd-mass nuclei, as well as even, can also be grouped into rotational bands was not so readily apparent from available nuclear data in 1953. γ spectroscopy at that time had insufficient resolution to sort out rotational structure, and high-resolution α spectroscopy on ^{241}Am, ^{239}Pu, and ^{231}Pa then showed a large density of levels near ground, with quite irregular patterns of α population. Bohr's 1952 paper[2b] supported the idea that the levels of odd-A-nuclei might be grouped into different interlaced rotational bands starting with a band head of some half-integral spin value I_0 and proceeding up by successive half-integral values with energies $(h^2/2J)[I(I + 1) - I_0(I_0 + 1)]$, where J is a moment of inertia. The interpretation of these complex spectra in odd-mass nuclei has relied more heavily on information from intensity patterns. An early aid was the idea[11] that there should be one band in the daughter that is populated with about the reduced[12] intensity of ground bands of neighboring even nuclei; such more intense band would be the one in which the orbital of the odd nucleon in the deformed potential did not change and the helium ion emission involved only the paired neutrons and protons. The other bands, where the state of the odd nucleon changed, would be more hindered. These ideas facilitated the classification of the low-lying levels of ^{237}Np formed in ^{241}Am α decay into two interlacing bands with band-head spins of $^5/_2$ and with opposite parities.[11] The detailed inter-

(2) (a) A. Bohr and B. R. Mottelson, *Kgl. Dan. Vidensk. Selsk., Mat.-Fys. Medd.,* **27,** No. 16 (1953); (b) A. Bohr, *ibid.,* **26,** No. 14 (1952).

(3) F. Asaro, F. L. Reynolds, and I. Perlman, *Phys. Rev.,* **87,** 277 (1952).

(4) T. Huus and C. Zupancic, *Kgl. Dan. Vidensk. Selsk., Mat.-Fys. Medd.,* **28,** No. 1 (1953).

(5) J. R. Arnold and T. Sugihara, *Phys. Rev.,* **90,** 332 (1953).

(6) K in deformed nuclei, as in diatomic molecules, stands for the projection of total angular momentum along the long axis.

(7) F. S. Stephens, R. M. Diamond, and I. Perlman, *Phys. Rev. Letters,* **3,** 435 (1959).

(8) (a) H. Morinaga and P. C. Gugelot, *Nucl. Phys.,* **46,** 210 (1963); (b) N. L. Lark and H. Morinaga, *ibid.,* **63,** 466 (1965).

(9) F. S. Stephens, N. L. Lark, and R. M. Diamond, *ibid.,* **63,** 82 (1965).

(10) M. Baranger and R. A. Sorensen, *Sci. Am.,* **221,** 58 (1969).

(11) J. O. Rasmussen, *Arkiv Fysik,* **7,** 185 (1953).

(12) "Reduced" here means that the rate dependence on the tunneling factor through the Coulomb barrier has been taken out.

pretation of ^{239}Pu spectra was somewhat delayed until the understanding of "anomalous" spacings of bands with projection quantum number $K = \frac{1}{2}$. In such bands the odd particle may be partly or wholly (if in an $s_{1/2}$ or $p_{1/2}$ orbital) decoupled from the rotating field of the even core, and the level energies consequently are not simply proportional to $I(I + 1)$, the quantum mechanical square of the angular momentum.

Bohr, Fröman, and Mottelson[13] soon gave a quantitative basis for the rotational intensity pattern to members of the strongly populated band (designated by them "favored decay") in odd-mass α decay. They suggested that the relative amplitudes C_l of α decay with the various orbital angular momenta C_0, C_2, C_4, etc., could be taken as the average of the two adjacent even neighbors in α decay to the ground band. With the l mix thus established, they showed from simple geometrical considerations that a given l wave will divide itself across various members of the daughter rotational band proportional to the square of a vector coupling (Clebsch–Gordan) coefficient $(lI_i 0K|IK)$ where I_i and I are initial and final spins, respectively, and K is the projection of the nuclear spin on the major axis of the prolate nuclear spheroid.

Thus, for favored bands of odd-mass nuclei

α decay intensity to band member with spin $I =$

$$\sum_l C_l^2 P_l(E_\alpha I)(lI_i 0K|IK)^2 \quad (1)$$

where $P(E_\alpha I)$ is the Coulomb barrier penetrability factor. The formula should be exact in the limit of small rotational energy spacing or vanishing quadrupole moment. Actually it is satisfied quite well throughout the region of actinide α emitters, with only a few exceptions which are understood by including additional interactions.

B. Determination of K Quantum Number by Branching. The Clebsch–Gordan branching formula then may be used to test the goodness of the K quantum number, and in this application the branching of γ or β transitions into a rotational band often provides a sharper test of K. With γ and β radiation, where the wavelengths of emitted photon or particles (electrons and neutrinos) are at least an order of magnitude greater than the nuclear size, the radiation usually proceeds by the lowest allowed multipolarity or angular momentum. (α decay, on the other hand, with the short wavelength of the emitted massive helium nucleus, exhibits extensive admixture of various l values.)

The branching relations for dipole radiation ($l = 1$) have long been known and applied in molecular spectroscopy, though usually in algebraic form and not in the Clebsch–Gordan formalism. Often the K value for a band can be trivially determined, since it usually equals the spin of the band-head level. Sometimes this is not the case.

For example, if the band-head spin equals 1, the K assignment is uncertain, and the transition branching

test is uniquely valuable. When a spin-1 state decays by $l = 1$ (dipole γ or $L = 1$ β decay) to ground (spin 0) and first excited state (spin 2) of an even–even nucleus, which of the two possible K values 0 or 1 does the initial state possess? The ratio of squares of the vector coupling coefficients tell us that, if $K = 0$, the spin-2 final state should be favored by a factor of two, whereas, if $K = 1$, the spin-0 final state is favored by a factor of two, and many examples of each are known.

C. Quantitative Deduction of Helium Ion Location on the Nuclear Surface before Barrier Penetration in α Radioactivity. As we mentioned earlier, there is seldom a significant mixing of L values in γ and β transitions, since the relevant wavelengths of these radiations always exceed nuclear dimensions by at least an order of magnitude. (Muon capture, a form of β decay, is an exception.) With such long wavelengths we would not expect these processes to reveal much about which regions of the nucleus contribute most to the transition. We must look to processes such as α decay or nuclear reactions, where wavelengths are short, to provide such detailed information.

The experimental intensity patterns of α decay to ground rotational bands of even nuclei presented an interesting challenge with the recognition[2a,11] in 1953 of the rotational nature of the levels. From the lightest deformed α emission with thorium parents to the heaviest known, the $L = 2$ intensities relative to the dominant $L = 0$ decrease monotonically with mass number. The $L = 4$ intensities decrease more rapidly to nearly vanish near ^{244}Cm decay and then increase for heavier nuclei. After some manipulations of the rather formidable expressions for coupling two angular momenta (α-orbital and nuclear rotational) in the laboratory frame, we found they reduced to quite simple formulations in the frame of a coordinate system fixed in the spheroidal nucleus.[14a] In this body-fixed frame in the limit of small rotational spacing the intensities of the various α groups to $I = 0, 2, 4, 6$ rotational levels are merely the squares of Legendre expansion coefficients of the angular wave function outside the Coulomb barrier. We thus could determine boundary conditions at large distance from experimental intensities and integrate the Schrödinger equation inward to the nuclear surface.[14] The procedure is subject to a sign ambiguity. Just as the X-ray crystallographer must guess a sign for the diffraction spots on his film, so also are our α intensities the squares of amplitudes which may have two possible phases. Figures 1 and 2 show the possible "snapshots"[14b,15] of the α wave function on the spheroidal nuclear surface, based on different phase choices. Like the X-ray crystallographer we must have some model to guide us to a proper choice of possible cases. It seemed likely that the α particle probability on the surface should be large in those zones where the wave functions of the most lightly bound nucleons were large,

(13) A. Bohr, P. O. Fröman, and B. R. Mottelson, *Kgl. Dan. Vidensk. Selsk., Mat.-Fys. Medd.*, **29**, No. 10 (1955).

(14) (a) J. O. Rasmussen and B. Segall, *Phys. Rev.*, **103**, 1298 (1956); (b) E. M. Pennington and M. A. Preston, *Can. J. Phys.*, **36**, 944 (1958).

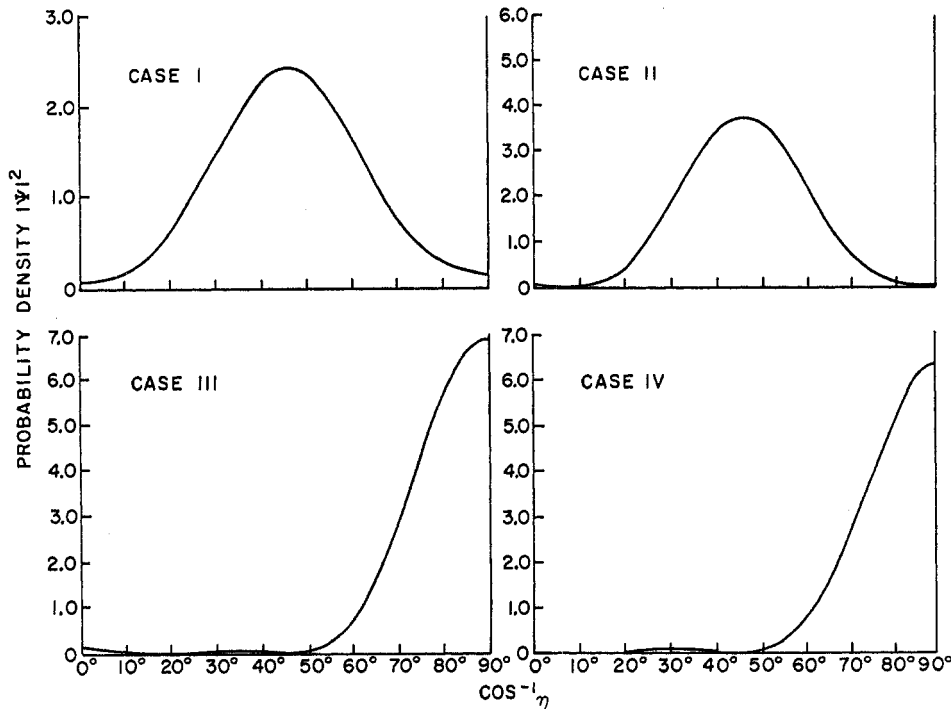(15) J. O. Rasmussen, *Rev. Mod. Phys.*, **30**, 424 (1958).

Figure 1. Theoretical[14b] α-particle probability density on the spheroidal nuclear surface for [242]Cm decay consistent with the experimental population of the lowest three levels of the ground band. The various cases represent the possible different assumptions for relative signs of transition amplitudes to the three levels ($I = 0, 2, 4$). Later work with a microscopic theory[22a] would suggest that case I or case II is the true case. The abscissa is defined in terms of prolate spheroidal coordinates, but it is essentially the polar angle.
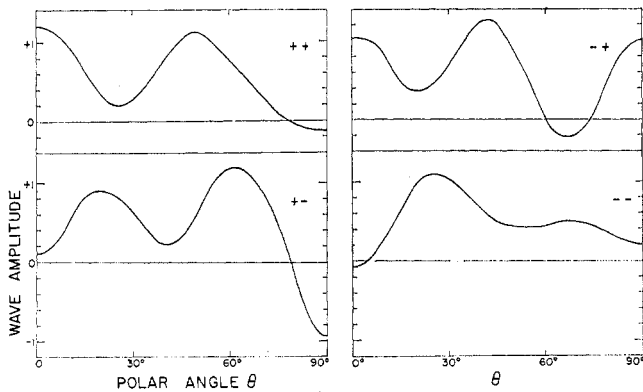
Figure 2. Theoretical[15] α-particle probability amplitude based on the phase choice of case I of Figure 1 but extended to take into account also the population intensities of the fourth ($I = 6$) and fifth ($I = 8$) band members. These four detailed subcases of case I (Figure 1) are labeled by the sign assumed for $I = 6$ and 8 amplitudes (relative to the band-head transition $I = 0$).

since these nucleons are the constituents from which the α particle must be formed. The normal order of filling particles of a particular oscillator shell into a prolate spheroidal potential well is as follows: first those orbitals extending along the long axis into the polar regions will be filled, then those in middle latitudes, and finally those in the equatorial zone. This qualitative picture was sufficient to eliminate cases III and IV of Figure 1. The quantitative microscopic[16] verification of this picture had to wait on other theoretical developments, good nucleonic orbital wave functions,[17,18] a

microscopic theory for α particle formation by Mang,[19] and a tractable theory for the pairing correlation between nucleons in nuclei.[20] Figure 3 shows the first published results (1962) of microscopic α theory of rotational population patterns.[21] Subsequent refinements of the theory[22] have provided increased confidence but have not appreciably altered numerically the results of Figure 3. These results are readily applicable to favored decay of odd-mass nuclei.

It is all very well to have a theoretical understanding of the trends of intensity patterns of favored decay, but these trends are so regular that simple extrapolation and interpolation of empirical curves has almost as much predictive value as the highly involved microscopic theoretical calculations requiring hours of time on high-speed computers. Hence, it is in the extension of microscopic α theory to the weak or "hindered" decays of odd-mass nuclei that the predictive value of the rate theory is best appreciated. The intensity patterns of hindered decay exhibit great variety and depend predominantly in the theory on the wave functions of the odd nucleon in the parent and in the daughter.[22b] The α particle wave function at the surface may be roughly

(16) By "microscopic" we mean treatments with their basis the product wave functions of nucleons moving in orbitals of the average field.

(17) S. G. Nilsson, Kgl. Dan. Vidensk. Selsk., Mat.-Fys. Medd., 29, No. 16 (1955).

(18) B. R. Mottelson and S. G. Nilsson, Kgl. Dan. Vidensk. Selsk., Mat.-Fys. Skr., 1, No. 8 (1959).

(19) H. J. Mang, Phys. Rev., 119, 1069 (1960).

(20) A. Bohr, B. R. Mottelson, and D. Pines, ibid., 110, 936 (1958); S. T. Belyaev, Kgl. Dan. Vidensk. Selsk., Mat.-Fys. Medd., 31, No. 11 (1959).

(21) H. J. Mang and J. O. Rasmussen, "Proceedings of the Rutherford Jubilee International Conference, Manchester, 1961," Heywood and Company, Ltd., London, 1961, p 561.

(22) (a) H. J. Mang and J. O. Rasmussen, Kgl. Dan. Vidensk. Selsk., Mat.-Fys. Skr., 2, No. 3, (1962); (b) J. K. Poggenburg, J. O. Rasmussen, and H. J. Mang, Phys. Rev., 181, 1697 (1969).
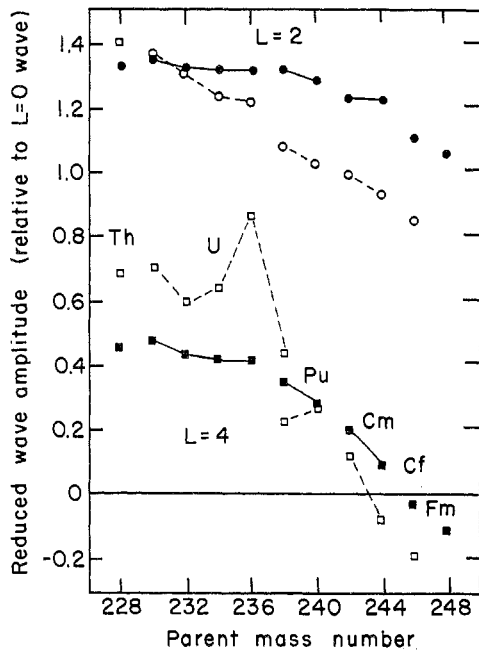
Figure 3. Experimental (open symbols) and microscopic theoretical (closed symbols) relative wave amplitudes for α decay to first excited (spin 2) and second excited (spin 4) rotational band members.
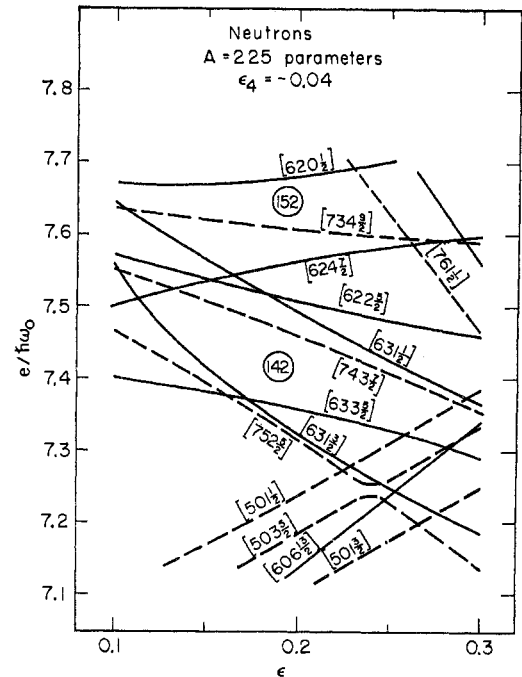
Figure 4. Energy level diagram[24] for neutrons in an elongated potential well appropriate to actinide nuclei. The abscissa is a quadrupole deformation parameter (essentially the fractional excess of semimajor axis over semiminor), and a fixed constant amount of the higher order 2^4-pole deformation is present. The ordinate is the orbital energy in units of the quantum energy $\hbar\omega_0$ for a neutron in a spherical harmonic oscillator potential of nuclear dimensions. The orbitals are labeled according to the Nilsson asymptotic quantum numbers defined in footnote 25. The subshells of larger spacing at 142 and 152 neutrons are specially indicated.

understood as the overlap of these two wave functions, though our calculations did not make this approximation. At the 20–30% eccentricities of the nuclear shape for most deformed α emitters the nucleonic orbitals are a rather complicated hybridization of various angular moments. The complete tabulation of several hundred theoretical α amplitudes has been published by Poggenburg, et al.[22b] We show here two examples of the unique predictive value of this work.

Baranov and coworkers[23] by high-resolution α spectroscopy on ^{239}Pu identified two weakly populated bands (α intensities $\sim 10^{-5}$ of the main α group), both of which had band-head levels of angular momentum $^5/_2$ and even parity. There were two logical candidates among the neutron orbitals for these assignments, the $^5/_2+$ orbital that constitutes the ground state of ^{233}U and ^{231}Th and the $^5/_2+$ orbital that becomes the ground band later at ^{241}Pu and ^{243}Cm. Both orbitals are mainly mixtures of $g_{9/2}$ and $i_{11/2}$ in, of course, orthogonal linear combinations. Figure 4 is a section of the correlation diagram calculated by Nilsson[24] showing neutron orbitals for actinides. The lower of these orbitals is to be seen in Figure 4 just below the $N = 142$ subshell, labeled [633 $^5/_2$].[25] The upper orbital $^5/_2+$ is half-

way between the subshells at 142 and 152 and is labeled (622 $^5/_2$). Detailed examination of the realistic wave functions of the particle in a deformed potential shows considerable admixtures of s, d, g, and i states in the parent ^{239}Pu state (631 $^1/_2$), and admixtures of d, g, and i states in the two $^5/_2+$ daughter state possibilities. Refer to Figure 13 in the Appendix for the actual positions of these $^5/_2+$ bands discussed here. Thus, the α amplitudes calculated by theory may include even values of orbital angular momenta (l_α) of 2 through 12, the allowed vector couplings of parent and daughter angular momenta. The theoretical calculations of Poggenburg, et al.,[22b] predict strongly differing α decay properties to these $^5/_2+$ bands, the (633 $^5/_2$) being much weaker. The mixture of l_α values is somewhat different, resulting in a different rotational band population "signature." Using the theory it is thus easy to assign these bands in the ^{235}U daughter to the Nilsson states. Figures 5 and 6 show comparisons of theory and experiment, essentially as the α particle probabilites on the nuclear surface, before barrier penetration.

Another useful application of the α theoretical signatures of population was made for weak α decay groups of ^{241}Am decaying to ^{237}Np. There the α signature and level spacings of an excited $K = ^1/_2$ band with spin $^3/_2$ band head at 267.54 keV was so irregular that the various α groups observed by Baranov, et al.,[26] were not initially recognized even as populating a single rota-

(23) S. A. Baranov, V. M. Kulakov, and S. N. Belenky, Nucl. Phys., 41, 95 (1963).

(24) S. G. Nilsson, "Nuclear Structure, Fission, and Superheavy Elements," Cargese Summer School Lectures, University of California Radiation Laboratory Report UCRL-18355, 1968.

(25) The labels are the so-called asymptotic quantum numbers, actually the quantum numbers of the cylindrical coordinate system for the anisotropic harmonic oscillator potential at large anisotropy. The numbers are [N, n_z, Λ, Ω], where N is the principal oscillator quantum number, n_z is the oscillator quantum number along the z axis of cylindrical symmetry, Λ is the projection of orbital angular momentum on the z axis, and Ω ($=K$) is the projection of total nucleonic angular momentum (orbital plus intrinsic spin) on the z axis. The intrinsic spin projection of $\pm^1/_2$ is equal to $\Omega - \Lambda$ and is sometimes designated as Σ.
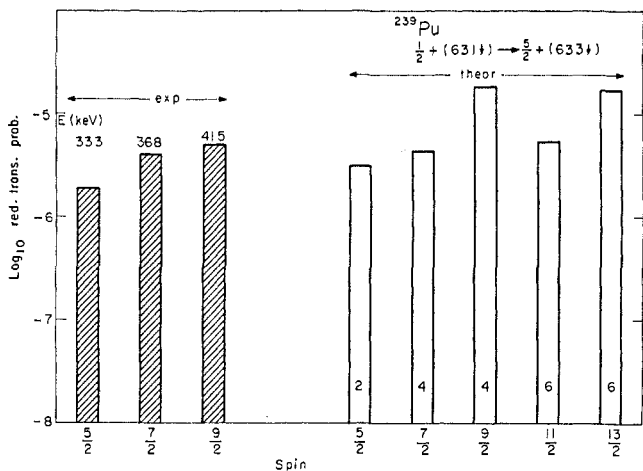
Figure 5. Experimental and microscopic theoretical[22b] transition intensity pattern to various rotational states for α decay of [239]Pu where the orbital of the odd neutron changes to the $5/2+$ (633).
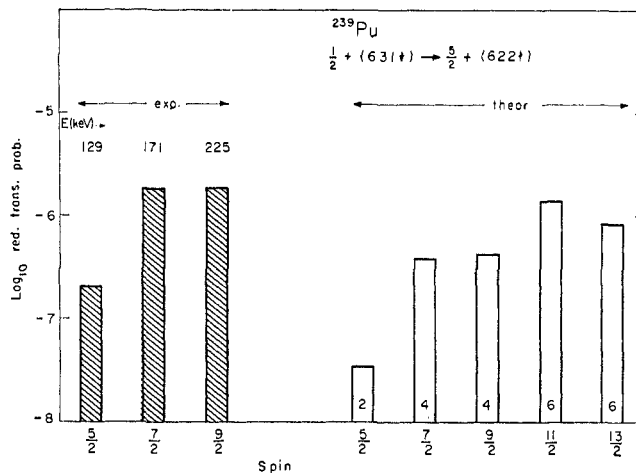

Figure 6. Experimental and microscopic theoretical[22b] transition intensity pattern to various rotational states for α decay of [239]Pu where the orbital of the odd neutron changes to the $5/2+$ (622).

tional band. The account of the use of α decay theoretical signatures and the latest spectroscopic information to sort out this band is related by Lederer, et al.[27] Figure 7 is from this work and shows the final set of rotational bands. Thus, starting with the Nilsson wave functions for nucleons in spheroidal potentials, a satisfactory microscopic α decay rate theory has been constructed and applied to real nuclei. There is, of course, much room for further work. Band mixing from the Coriolis force or from collective vibrational effects has not been treated, and the Coulomb barrier penetrability problem in the presence of electric quadrupole coupling needs more careful treatment.

III. Rotational Intensity Patterns in Nuclear Reactions

A. Multiple Coulomb Excitation, Inelastic Scattering at Energies below the Coulomb Barrier.

An important method for the study of ground rotational bands and the electric quadrupole matrix elements interconnecting states is multiple Coulomb excitation. Deformed target nuclei are bombarded with projectiles, ranging from carbon to argon, at energies below the Coulomb barrier for nuclear reactions. At such lower energies the complication of the short-range nuclear attractive force does not enter, and significant rotational inelastic scattering results only from the electric quadrupole interaction. Thus, this method, using protons and helium ions as projectiles, has been the most powerful general method of measuring nuclear quadrupole distortions, since the probability of exciting the first-excited rotational state is proportional to the square of the intrinsic quadrupole moment.

When yet heavier ions, such as argon, are fired at the nuclei, higher rotational states receive increasing populations. For example, pioneering work of Stephens, Diamond, and Perlman[7] showed that at argon energies

of 190 MeV the state with angular momentum 6 in uranium-238 is almost as heavily populated as the spin-4 state below it in the ground band.

The definitive theoretical work is that of Alder and Winther.[28] This article and other key articles in the development of Coulomb excitation are collected in book form.[29]

Multiple Coulomb excitation provides one of the few means of directly measuring the static quadrupole moments of 2+ first excited states. Such measurements within the region of rotational nuclei do not show deviation from simple theory. Outside the rotational region (in Sn, Cd, Te nuclei) there is considerable current interest in making such measurements,[30] and model predictions are less certain.

B. Rotational Inelastic Nuclear Scattering above the Coulomb Barrier.

If we raise the projectile energies above the Coulomb barrier, we enter a new region in which absorption and phase shifts at the deformed nuclear surface assume a dominant role compared to Coulomb excitation. Most nuclear projectiles, except protons and neutrons, are strongly absorbed in the nuclear surface, without regard to details of internal nucleon orbitals. Hence the patterns of inelastic rotational scattering offer a general means of measuring details of the shape of the nuclear surface.

Deuteron scattering on deformed rare-earth targets by Elbek, et al., gave inelastic cross sections smoothly falling off with angle.[31] He pointed out that certain features of the cross sections indicated P_4 ($\cos \theta$) shape terms besides the well-known quadrupole shape terms.

α particle bombardments at about twice the barrier energies by Harvey and collaborators[32] yielded a wealth

(26) S. A. Baranov, V. M. Kulakov, and V. M. Shatinsky, Nucl. Phys., 56, 252, (1964).
(27) C. M. Lederer, J. K. Poggenburg, F. Asaro, J. O. Rasmussen, and I. Perlman, ibid., 84, 481 (1966).

(28) K. Alder and A. Winther, Kgl. Dan. Vidensk. Selsk., Mat.-Fys. Medd., 32, No. 8 (1960).
(29) K. Alder and A. Winther, "Coulomb Excitation," Academic Press, New York, N. Y., 1966. Reference 7 is reprinted in this book.
(30) J. de Boer, R. G. Stokstad, G. D. Symons, and A. Winther, Phys. Rev. Letters, 14, 564 (1965).
(31) B. Elbek, M. Kregar, and P. Vedelsby, Nucl. Phys., 86, 385 (1966).
(32) B. G. Harvey, D. L. Hendrie, O. N. Jarvis, J. Mahoney, and J. Valentin, Phys. Letters, 24B, 43 (1967).

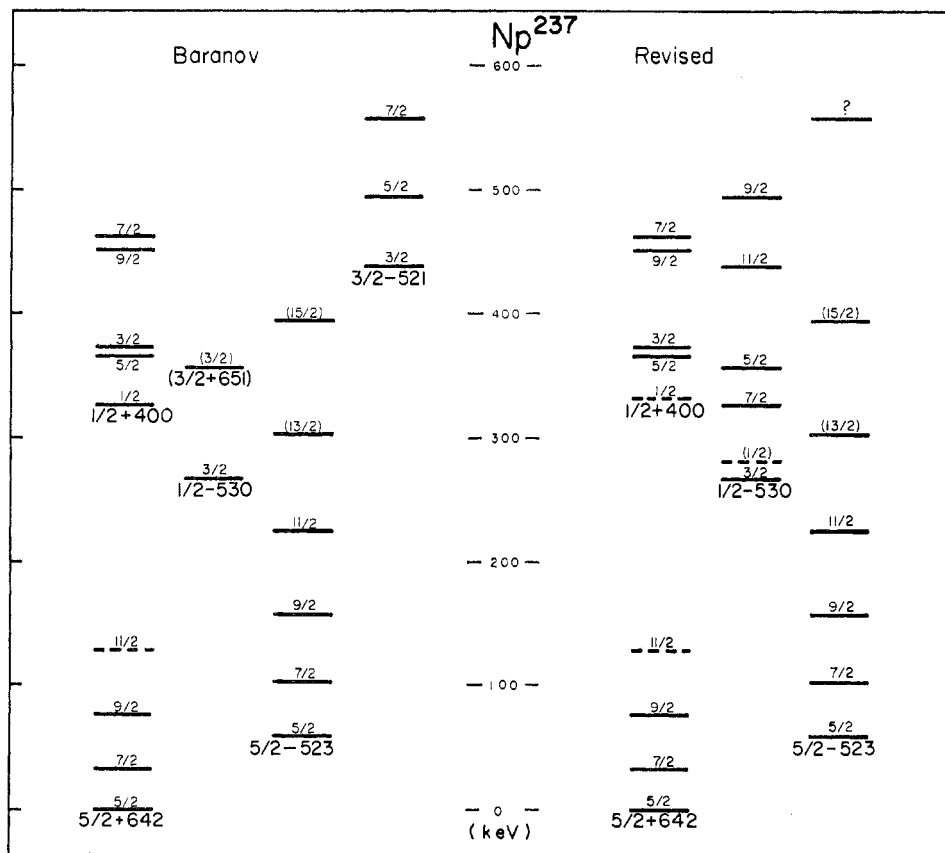Figure 7.   Rotational band scheme of ^{237}Np as deduced (left) from α-decay work and (right) after γ-ray work and application of α rate theory.

of information exhibited in a strong diffraction structure in angular dependence of the inelastic scattering cross section.   With Glendenning this group has fit results by extensive coupled-channel optical model calculations,[33] and they have convincingly extracted P_4 moments of the nuclear shape.   Their results indicate that deformed nuclei are not in general purely spheroidal; the shapes tend from a rounded diamond rotated about the long diagonal around samarium to rounded cylinders at the upper end of the rare-earth region.

C. Rotational Excitation in Rearrangement Collisions.   We turn now to the question of rotational excitation in nuclear collisions where one or more nucleons are exchanged between collision partners.   In contrast to inelastic scattering, the rotational excitation patterns of these transfer reactions may depend most sensitively on the details of the nucleon orbitals involved.   The most extensively studied reactions are the (d,p) and (d,t) where a bombarding deuteron loses or picks up a neutron.   Sheline first showed[34] that the rotational pattern using even–even deformed rare-earth targets ($I = 0$) has an especially simple interpretation.   The intensity of population of a rotational level, I, is directly proportional to the fraction of that angular momentum in the bound orbital of the transferred neutron.   Figure 8 is from Sheline's paper with Vergnes,

and one sees good correspondence with Nilsson's theoretical "hybridized" orbitals[17] in a spheroidal potential.   To extract these percentages from experiment one makes use of a distorted wave Born approximation (DWBA) to calculate the kinematic factors involved in transfer.   A recent detailed analysis by these methods is to be found in the work of Rickey, et al.[35]   See also Figure 13 in the Appendix for the impressive level scheme deduced by this method for ^{235}U.

The (d,p) and (d,t) reactions are poor for effecting large angular momentum transfers and thus do not very well probe the high angular momentum components in the neutron orbitals.   The recent work of Elze and Huizenga[36] shows the highly exothermic (^{3}He,^{4}He) reaction to be complementary to (d,p) and (d,t), particularly favoring these high angular momentum components.   For example, they find the above reaction on ^{236}U readily extracts a neutron to populate the $I = {}^{15}/_2$ level of the $K = {}^7/_2$ ground rotational band of ^{235}U, showing its character as predominantly a $j = {}^{15}/_2$, $M_j = {}^7/_2$ orbital.

The analogous transfer reactions for protons have lower cross sections because of the Coulomb barrier reduction of proton tunneling.   However, the (^{3}He,d) reaction looks promising as a probe of details of individual proton orbitals in the deformed nuclei.

(33) D. L. Hendrie, N. K. Glendenning, B. G. Harvey, O. N. Jarvis, H. Duhm, J. Saudinos, and J. Mahoney, *Phys. Letters*, 26B, 127 (1968).
(34) M. N. Vergnes and R. K. Sheline, *Phys. Rev.*, 132, 1736 (1963).

(35) F. A. Rickey and R. K. Sheline, *ibid.*, 170, 1157 (1968).
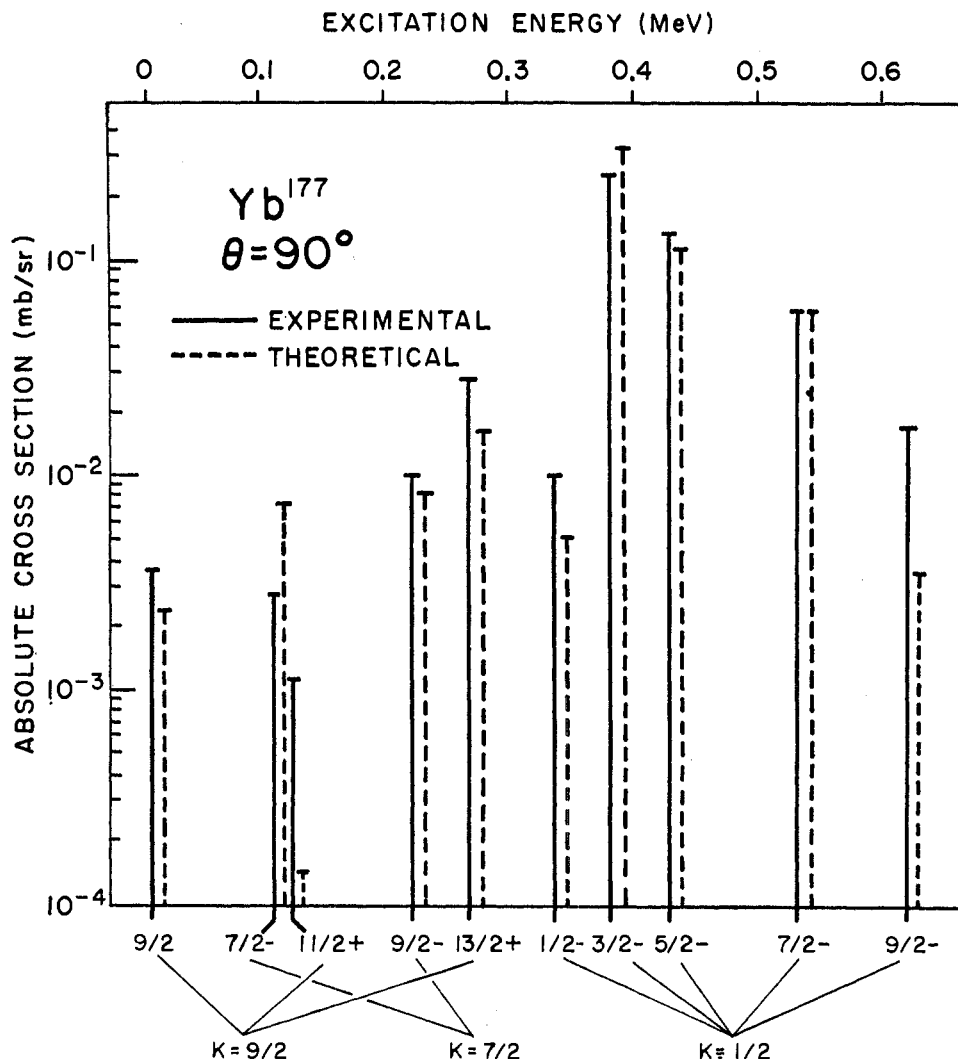(36) T. W. Elze and J. R. Huizenga, *Bull. Am. Phys. Soc.*, *Ser. II*, 14, No. 1, 57 (1969).

Figure 8. Comparison[34] of experimental (solid) and theoretical (dashed) cross sections for exciting various rotational band members in a neutron-transfer (d,p) reaction. The horizontal position of the bars gives the excitation energy of the level in the [177]Yb nucleus. The differential cross section is given in millibarns (10^{-27} cm^2) per steradian as observed at an angle of 90° to the incident beam.

D. Rotational Excitation in Complete Fusion Reactions. At bombardment energies well above the Coulomb barrier complete fusion of projectile and target nuclei is predominant with cross sections approaching the geometrical value πR^2. For rare-earth nuclei the main loss of excitation energy of the compound system comes by a statistical "evaporation" of neutrons on a 10^{-20}-sec time scale, followed by a slower cascade of γ rays. Pioneering work[8b] in Amsterdam with low-resolution sodium iodide spectroscopy showed already by 1962 the feasibility of measuring the ground rotational band transitions despite the myriad unresolved background transitions. The subsequent development of high-resolution lithium–germanium γ spectroscopy has made this in-beam observation of γ rays following (α,xn) or (heavy ion,xn) reactions a very general method for mapping rotational bands.

Some attempts[37] have been made to infer from rota-

tional population patterns the dependence of nuclear level densities on angular momentum. It appears, however, that simple statistical models for feeding the ground rotational band are inadequate and that feeding depends on details of the next higher bands serving as feeders. Qualitatively, the higher the average angular momentum in the compound system the more intensely the high-spin band members are fed.

E. Rotational Excitation in Fission. We pointed out in section C that the rotational population patterns in α decay provided "snapshots" of the α particle probability just inside the Coulomb barrier. So also should rotational populations in nuclear fission measure the state of bending motion of the egg-shaped fragments at the point of first separation.

A molecular analogy would be the breakup of a linear triatomic molecule. The rotational excitation of the diatomic product would be determined by the motion in the bending mode of the transition state.

We have considered events of fission where one fragment is spherical and have assumed a zero-point vibrational motion in the bending mode. Thus we have

(37) G. B. Hansen, B. Elbek, K. A. Hagemann, and W. F. Hornyak, *Nucl. Phys.*, **47**, 529 (1963); J. O. Rasmussen and T. T. Sugihara, *Phys. Rev.*, **151**, 992 (1966); C. F. Williamson, S. M. Ferguson, B. J. Shepherd, and I. Halpern, *ibid.*, **174**, 1544 (1968).
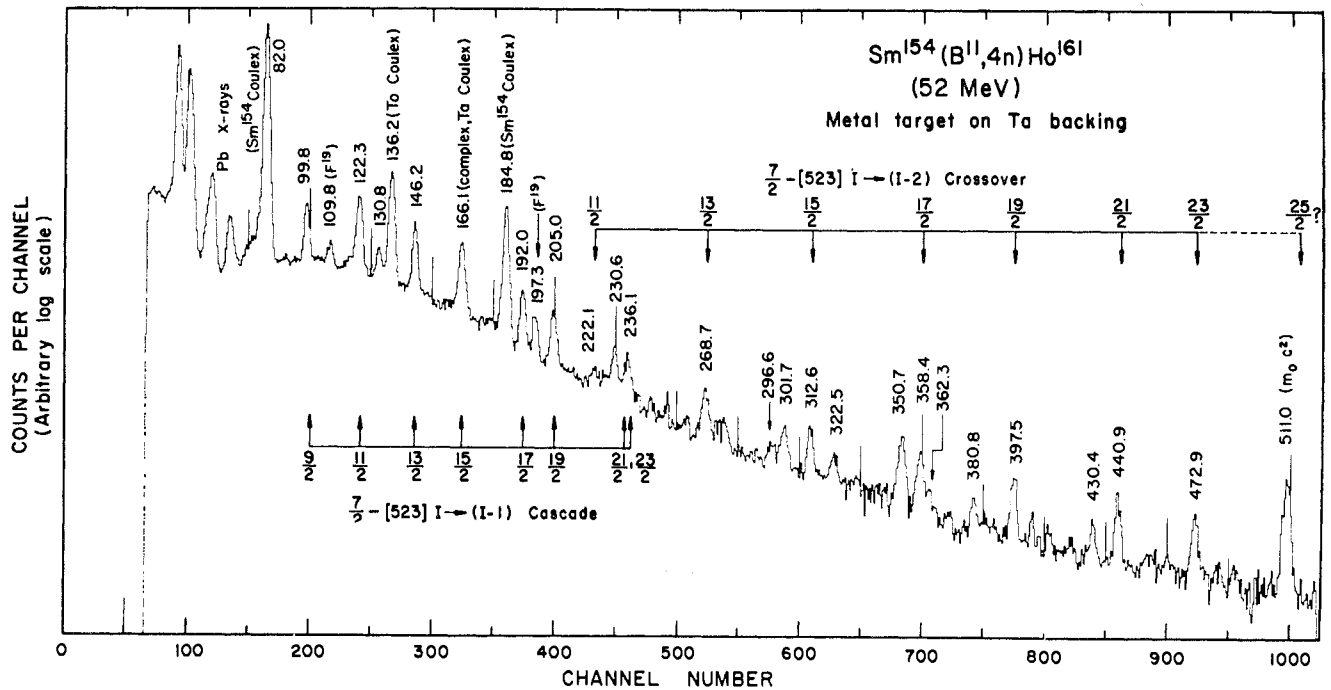
Figure 9. The γ-ray spectrum observed by a 15-cc lithium-drifted germanium detector with 52-MeV ^{11}B bombardment of ^{154}Sm. Transitions assigned to the ground rotational band of ^{161}Ho are especially indicated. Data are from studies[44] at the Yale heavy ion accelerator.
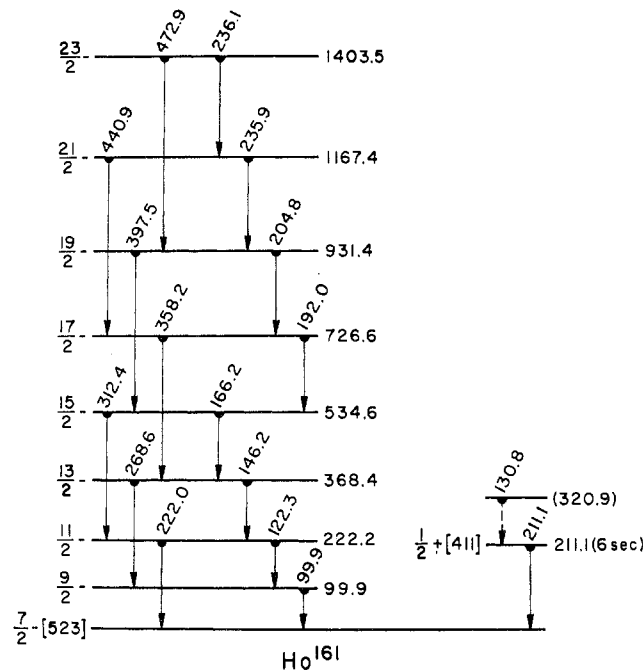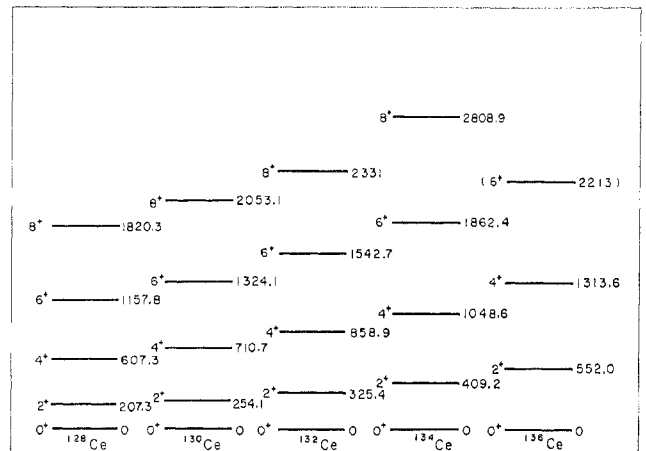

Figure 10. Partial level scheme of ^{161}Ho as deduced mainly from data shown in Figure 9. Levels are labeled on the left by angular momentum and parity and on the right by energy in kiloelectron volts. Asymptotic quantum numbers (see ref 17) are indicated by band heads.

estimated[38] the average rotational angular momentum of ^{108}Ru in thermal neutron fission of ^{239}Pu. This root-mean-square angular momentum theoretically is about seven units. Several experiments have attempted to deduce average angular momenta in fission based on γ

Energy levels in light Cerium nuclei

Figure 11. Energy level schemes of a series of cerium nuclei as determined at the Berkeley heavy ion linear accelerator (USAEC). The schemes were deduced[45] from γ-ray spectra following various heavy-ion-induced nuclear reactions.

angular distribution or isomeric yields, though no experiments have measured the mass 108 region. The experimental root-mean-square estimates of angular momentum are as follows: ~8 (mass 81, 83),[39] 6 (masses 131, 133),[40] ~7 (averaged over all masses),[41] and 8.4 (averaged over all masses).[42] The general agreement is satisfactory, but it will be good to have more experiments bearing on the question of rotational excitation of fission fragments.

(38) J. O. Rasmussen, W. Nörenberg, and H. J. Mang, *Nucl. Phys.*, **A136**, 465 (1969).

(39) I. F. Croall and H. H. Willis, *J. Inorg. Nucl. Chem.*, **25**, 1213 (1963).
(40) D. G. Sarantites, G. E. Gordon, and C. D. Coryell, *Phys. Rev.*, **138B**, 353 (1965).
(41) M. M. Hoffman, *ibid.*, **133B**, 714 (1964).
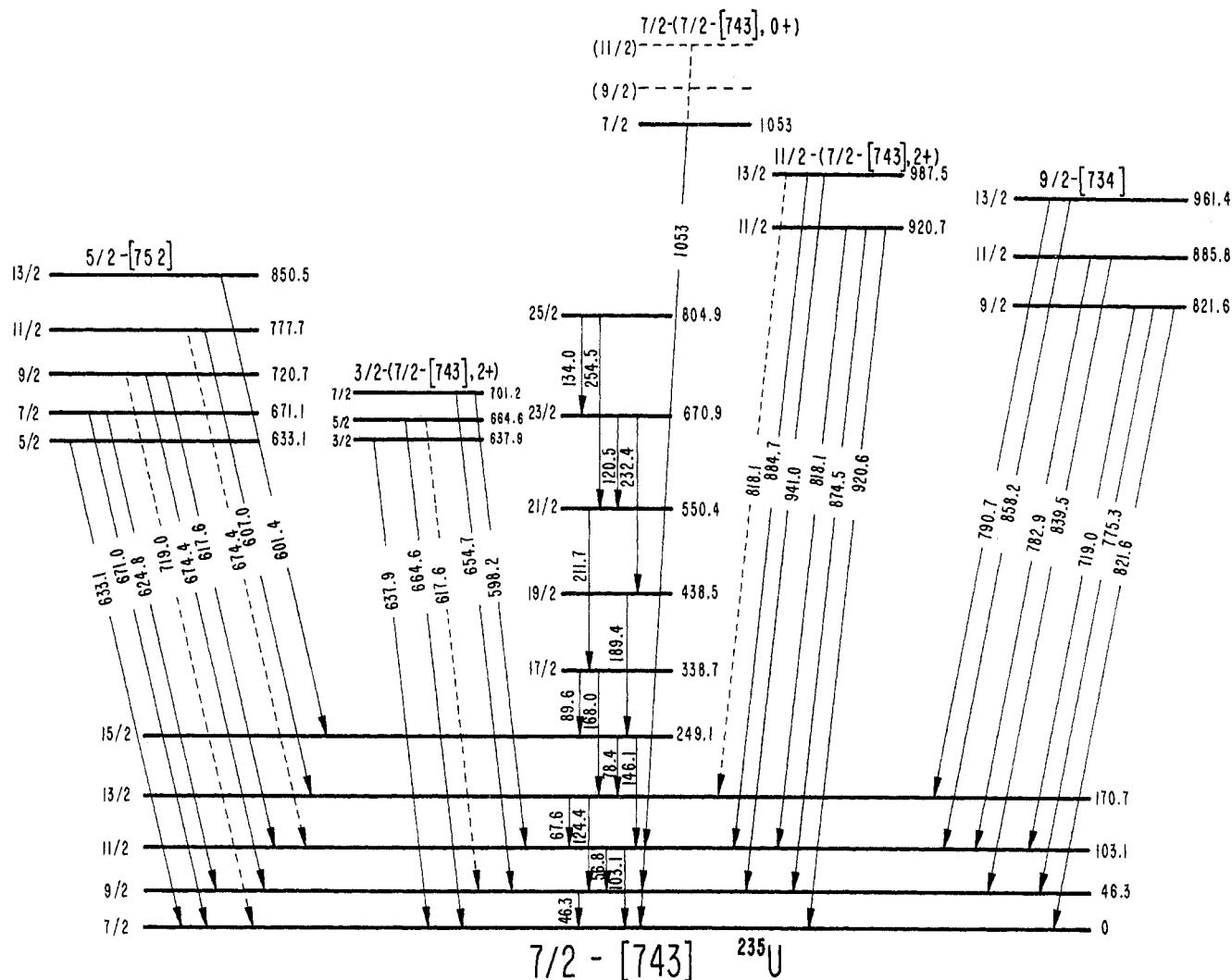(42) T. D. Thomas and J. R. Grover, *ibid.*, **159**, 980 (1967).

Figure 12. Energy levels and γ transitions in ²³⁵U as observed[46] in multiple Coulomb excitation by the ions ⁴He, ¹⁶O, and ³⁸Ar at energies too low to effect contact with the nuclear surface.

IV. Concluding Remarks

It may well turn out that the nuclear rotational studies and concepts will have increasing relevance to molecular collisions and ion–molecule interactions. Already some experiments, such as photoionization of gaseous hydrogen, have nearly resolved discrete rotational states.[43] It is to be hoped that improved measurements of rotational energy transfer in molecular reactions will bring these processes to a common ground with the analogous nuclear work.

Appendix. Representative Nuclear Spectra and Level Schemes

In the introduction was stressed the close analogy between nuclear and molecular processes exciting rotational motion. The spectral measurements involve entirely different equipment, since the energy scales differ so vastly. We may make a rough estimate of the scale factor change by noting that moments of inertia involve a sum of products of masses times the square of their

distances from the axis of rotation. The masses in molecular and nuclear cases are nearly the same, but the distances differ by ∼10⁵ (ångströms, 10⁻⁸ cm, vs. fermis, 10⁻¹³ cm). Hence, nuclear rotational spacings are some ten orders of magnitude larger than molecular. Whereas molecular rotational transitions usually lie in the microwave region, the pure rotational transitions of nuclei are in the region of hard X-rays, that is, tens of kilovolts. Spectrometers suitable for X-rays are applicable. In recent years lithium-drifted germanium diode devices, back-biased and cooled to liquid nitrogen temperature, have proved most powerful for spectrometry, since the electrical pulses following γ-ray absorptions show a close proportionality to energy. Figure 9 shows such a spectrum from recent reaction work at the Yale heavy ion accelerator. Figure 10 shows the level scheme of the ground rotational band in ¹⁶¹Ho as deduced from this spectrum. Note that the angular momentum values of the state take on successive half-integral values going up from a band head of angular momentum ⁷/₂. The analogous situation would apply to a diatomic molecule (radical) with an odd number of electrons. It is common in such nuclear bands that the collectively enhanced electric quadrupole transitions are competitive

(43) K. Siegbahn, et al., "ESCA, Atomic, Molecular, and Solid State Structure by Means of Electron Spectroscopy," Almqvist and Wiksells Boktryckeri AB, Uppsala, 1967, cf. p 209.
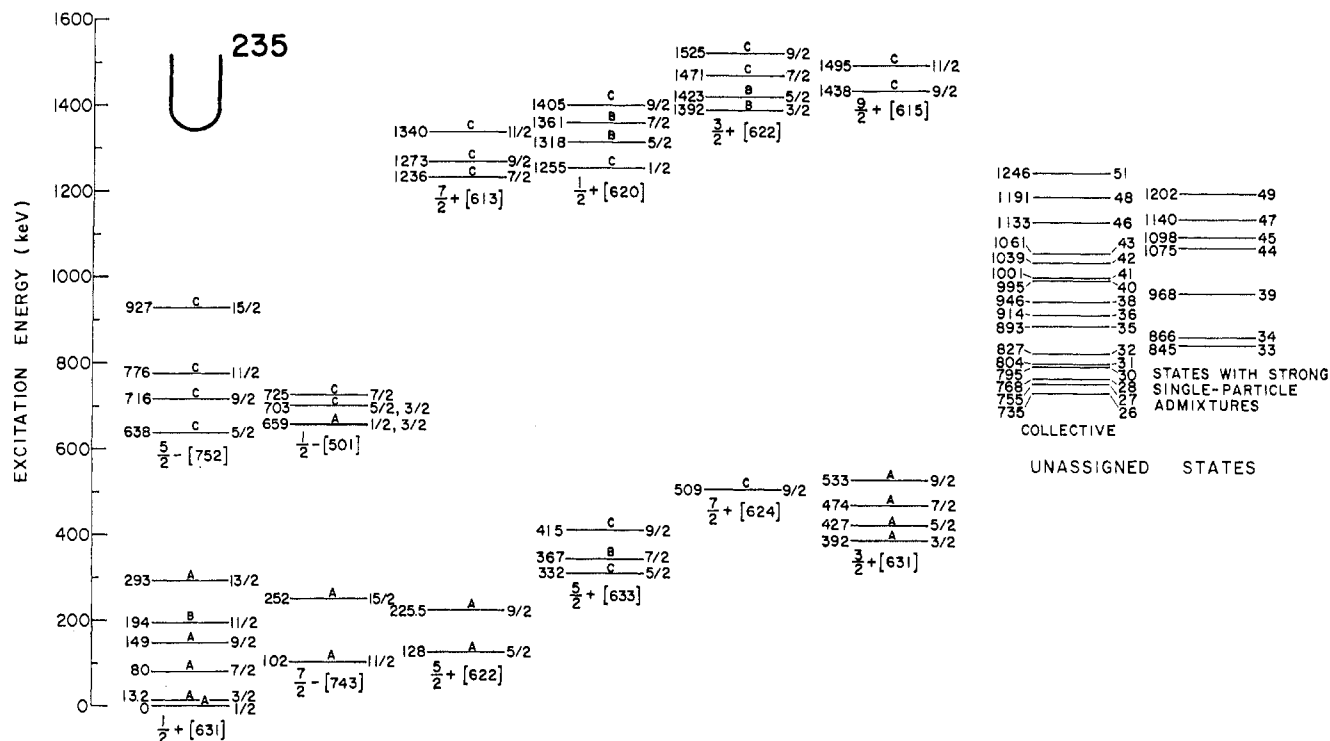
Figure 13. Energy levels of ^{235}U as measured[47] by neutron transfer to or from bombarding deuterons. This work from the Argonne National Laboratory tandem Van de Graaff accelerator involves high-resolution magnetic spectrographic measurement of the final light product (proton or triton).

in rate with magnetic dipole transitions. Thus, the typical radiative decay pattern for such a band is as shown in Figures 9[44] and 10, mixed dipole–quadrupole transitions cascading between adjacent levels and quadrupole transitions jumping across such that their energies equal the sum of two cascade transitions.

Figure 11, taken from work of Ward, Diamond, and Stephens,[45] shows a series of bands for various cerium nuclei, as measured also by γ-ray spectroscopy following reactions induced by oxygen and by neon ions. There is a gradual change from the lightest nucleus, ^{128}Ce, which may be regarded as truly deformed, through "transitional nuclei" to the spherical ^{136}Ce. This behavior is typical as the number of neutrons approaches the closed configuration of 82.

Finally, we show the extent of rotational band knowledge now available for ^{235}U. Figure 12 from work of

Stephens, Holtz, Diamond, and Newton[46] shows the band structure revealed by γ spectroscopy following multiple Coulomb excitation with helium, oxygen, and argon projectiles. This is the process discussed in section IIIA, where the projectiles have energies too low to make actual nuclear contact with target nuclei and excitation occurs via the electric field of the passing ion. The above studies have recently been complemented by work involving charged particle spectroscopy following transfer of a neutron, the rearrangement collisions discussed in section IIIC. Figure 13 from work of Braid, Chasman, Erskine, and Friedman[47] shows the levels of ^{235}U revealed by these studies, namely (d,p) reactions on ^{234}U and (d,t) on ^{236}U. Note that many levels are common between Figures 12 and 13, but others are found only by one of the processes.

(44) J. O. Rasmussen, J. Alonso, H. Bakhru, F. Bernthal, J. Boutet, and B. Olsen, 158th National Meeting of the American Chemical Society, New York, N. Y., Sept 1969, Abstract NUCL 53.

(45) D. Ward, R. M. Diamond, and F. S. Stephens, Nucl. Phys., A117, 309 (1968).

(46) F. S. Stephens, M. D. Holtz, R. M. Diamond, and J. O. Newton, ibid., A115, 129 (1968).

(47) A. M. Friedman, J. R. Erskine, T. H. Braid, and R. R. Chasman, 158th National Meeting of the American Chemical Society, New York, N. Y., Sept 1969, Abstract NUCL 77.